euspen's 26th International Conference & Exhibition, Krakow, PL, June 2026
www.euspen.eu

Fundamental Investigation of Cutting Mechanisms in Ultra-Precision Machining of KTP Crystals for Quantum Communication

E. Uhlmann[1,2], M. Polte[1,2], T. Hocke[1,2], T. D. Le[1]

[1]*Institute for Machine Tools and Factory Management IWF, Technische Universität Berlin, Germany*
[2]*Fraunhofer Institute for Production Systems and Design Technology IPK, Germany*

le@tu-berlin.de

Abstract
Quantum communication is a key technology for encryption and secure transfer of information, especially in times of highly sensitive data and digital security. Therefore, the use of entangled photons opens new possibilities in information transmission, as they are a fundamental resource of quantum mechanical methods and enable innovative approaches in quantum communication. Potassium titanyl phosphate (KTP) in its periodically poled form (ppKTP) is used as a source for entangled photons due to its nonlinear optical properties. Its inherent brittleness represents a significant limitation for crack-free ultra-precision machining of complex optics for quantum repeaters. Therefore, fundamental investigations of cutting mechansims in ultra-precision machining have been carried out. The ultra-precision planing tests have been carried out on a machine tool of type 650 FG v3 manufactured by Moore Nanotechnology Systems, USA, equipped with nanopolycrystalline diamond (NPD) cutting tools from A.L.M.T. Corp., Japan. The lowest arithmetic mean height Sa = 0.89 nm and arithmetical mean deviation Ra = 0.76 nm were achieved at a depth of cut a_p = 2.5 µm, a cutting speed of v_c = 50 mm/min and a width of cut a_e = 1.5 µm, using a tool with a corner radius r_ε = 400 µm and a cutting edge radius r_β < 1 µm. With decreasing width of cut, both the number of micro-cracks and the fracture width decreased. In conclusion, the influence of the width of cut and the corresponding undeformed chip thickness on the micro-crack and fracture characteristics of KTP was clarified.

Keywords: hard-brittle materials, nanopolycrystalline diamond tool, ultra-precision machining

1. Introduction

Quantum computers are increasingly important for social and technological development, whereby the optimization of information transmission is also becoming a growing priority. In particular, the use of quantum mechanical interactions offers new application possibilities with far-reaching societal significance. Thus, the field of quantum communication emerged with the approach of transmitting information using entangled photons, representing an important milestone in information security.

Potassium titanyl phosphate (KTP) crystals are used for photonic applications, as periodic poling potassium titanyl phosphate (ppKTP) enables efficient nonlinear optical processes [1]. In addition to suitable optical properties, precise mechanical machining of the crystal is also essential. In this context, this work investigates machining with geometrically defined cutting edges for the machining of the brittle material ppKTP in order to achieve ultra-precision surface qualities and shape accuracy a_s. According to the state of the art, crystals such as ppKTP are primarily machined using tools with undefined cutting edges, such as grinding and polishing [2]. However, these approaches are limited by a curvature radius of r_f < 10 mm. In addition, process-related grooves occur that alter the optical properties of the component and would therefore impair the functionality of the crystals [3]. Consequently, machining with geometrically defined cutting edges, in particular UP-planing and -turning, represent a novel approach for machining of ppKTP materials. For this reason, the overall objective is the realization of UP-planing and -turning of ppKTP for the use of quantum optics. Due to the brittle properties of the ppKTP crystal, machining strategies are required that enable material removal with ultra-precision surface roughness and shape accuracy a_s.

According to the state of the art, this is achieved for brittle materials when a hydrostatic compressive stress state is present [4] as well as the critical undeformed chip thickness h_{crit}, which defines the brittle-to-ductile transition, is not exceeded [5]. Recent investigations showed that ultra-precision machining of ppKTP crystals with sufficient surface roughness and shape accuracy a_s, including their periodically poled form, was achieved using a nanopolycrystalline diamond (NPD) tool, as its applicability was previously demonstrated for brittle materials such as cemented carbide [6]. In the present study, the employed NPD tools have a cutting edge radius of r_β < 1 µm and a corner radius of r_ε = 0.4 mm [7]. Under these conditions, crack-free material removal without the occurrence of brittle fractures was observed for depths of cut of a_p < 4 µm. For this purpose, scratching experiments with increasing depths of cut a_p were conducted to analyse the influence of the depth of cut a_p on surface formation and to identify the respective cutting regimes [7]. While these investigations clarified the influence of the depth of cut a_p, the scratch-based methodology involves continuously varying process conditions, preventing an isolated evaluation of the local undeformed chip thickness h and its direct correlation with surface quality. To address this research gap, the present study proposes partial-cut planing experiments as an analogous approach to enable the isolated investigation of the influence of the undeformed chip thickness h on surface formation. This allows for a systematic variation of the undeformed chip thickness h, while maintaining constant cutting conditions in terms of depth of cut a_p, width of cut a_e and cutting speed v_c, thus enabling a clear correlation between the undeformed chip thickness h, material removal mechanisms and the resulting surface roughness.

2. Experimental setup and methodology

In this study, a KTP-crystal from the company EKSMA Optics, UAB, Vilnius, Lithuania, was used in its original form without periodic poling, due to the high availability and lower cost compared to ppKTP-crystals. While the crystal structure remains unchanged, the optical properties are modified by the poling process [8], as periodic poling is regarded as a functional post-processing step for nonlinear crystals such as KTP. Therefore, the same material-specific machining behaviour applies.

To identify ranges of the undeformed chip thickness h associated with reduced brittle damage, ten grooves were machined. For each groove, a constant width of cut a_e was applied, while varying values were assigned between grooves, ranging from $a_e = 0.5$ µm to $a_e = 5$ µm in increments of $a_e = 0.5$ µm. The depth of cut was kept constant at $a_p = 2.5$ µm, since ductile machining was demonstrated for the employed tool at this value [7]. Likewise, the cutting speed was kept constant at $v_c = 50$ mm/min according to Uhlmann et al. [7] to achieve an isolated investigation of the influence of the width of cut a_e and the resulting maximum undeformed chip thickness h_{max}, which can be determined due to the formation of the comma-shaped chip according to Equation (1) [9]:

$$h_{max} = r_\varepsilon - \sqrt{r_\varepsilon^2 + a_e^2 - 2\, a_e \sqrt{2\, r_\varepsilon\, a_p - a_p^2}} \qquad (1)$$

As a result, widths of cut of 0.5 µm ≤ a_e ≤ 5.0 µm corresponds to a range of maximum undeformed chip thicknesses of 55.01 nm ≤ h_{max} ≤ 527.24 nm. The grooves were machined completely over the entire length of cut l = 4 mm under dry conditions, resulting in a groove width of w = 0.1 mm. Table 1 summarises the applied planing parameters.

Table 1 Process parameters for the planing process

Parameter	Symbol	Value
depth of cut	a_p	2.0 µm
cutting speed	v_c	50.0 mm/min
width of cut	a_e	0.5 µm - 5.0 µm
cooling lubricant	-	dry machining

2.1 Machine technology

The experiments were conducted using a 5-axis ultra-precision machine tool type 650 FG v3 manufactured by the company Moore Nanotechnology Systems, Swanzey, USA. Due to its climate-controlled working environment and the granite machine bed, stable thermal conditions and low vibration levels are ensured. In particular, the aerostatic and hydrostatic bearings of the spindle and linear axes enable slip-stick-free motions, allowing surface qualities in the sub-nanometer range to be achieved.

2.2 Tool geometry and measurement methods

For the experiments, NPD-tools from the company A.L.M.T. Corp., Tokyo, Japan, were used, featuring a corner radius of $r_\varepsilon = 0.4$ mm, a cutting edge radius of $r_\beta < 1$ µm. The grooves were machined with a rake angle of $\gamma_0 = 0°$.

The same type of tool with comparable specifications was employed in the scratching tests conducted by Uhlmann et al. [7] to determine the critical depth of cut $a_{p,crit}$.

To quantify the data, the planed surfaces were measured using a white light interferometer (WLI) type Zygo NewView 5010 from the company Ametek Germany GmbH, Weiterstadt, Germany, in which the surface roughness Sa was determined. Furthermore, the topographical examination of the grooves and the characterisation of the initial tool condition were performed using a ZEISS LEO 1455 VP scanning electron microscope (SEM) from the company Leica Electron Optics, Wetzlar, Germany. The initial tool condition is shown in Figure 1.

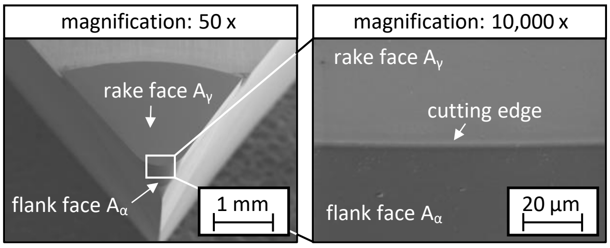

Figure 1. SEM image of the initial condition of the NPD-tool

The tool was geometrically characterised using a focus variation microscope type InfiniteFocus manufactured by Alicona Imaging GmbH, Graz, Austria, to determine the cutting edge radius r_β. To examine the occurring process forces F_P during the planing process, a 3-component dynamometer of the type Kistler 9256C2 from Kistler Instrument AG, Winterthur, Switzerland, was used.

3. Cutting results

Since the grooves were machined on the free surface of the material, three distinct regions can be identified: full-cut region, partial-cut region and the region of comma-shaped chip formation, as exemplarily illustrated for a single groove with a width of cut of $a_e = 3$ µm in Figure 2.

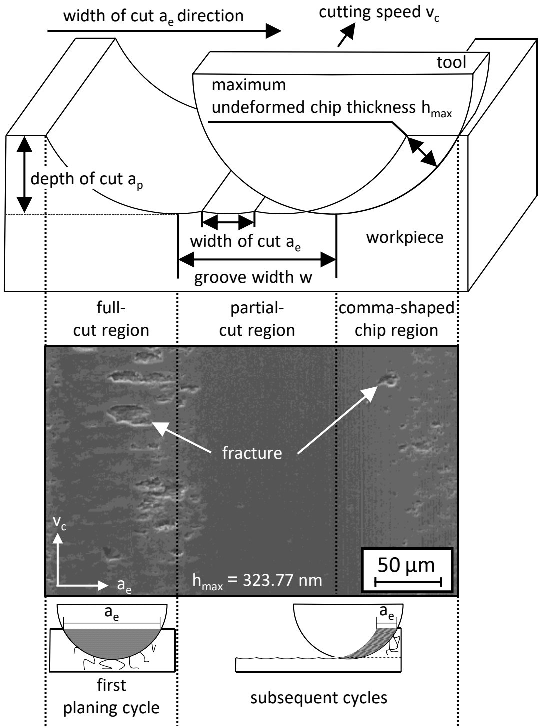

Figure 2. Schematic illustration of the planing process and resulting surface regions shown in a SEM image

The full-cut region corresponds to the first planing cycle and is characterised by continuous fractures that are observed in all grooves. This is expected, as the full-cut condition is solely defined by the cutting speed v_c and depth of cut a_p, which are identical for all grooves. The largest fractures originate at the groove bottom and decrease towards the edge, as the brittle regime is first reached at the groove bottom in the full-cut region. In contrast, the partial-cut region begins from the second planing cycle. Due to the reduced chip cross-section A in the partial-cut region, the material removal mechanism changes, resulting in a distinctly different surface formation compared to the full-cut region and leading to altered cutting forces F_c. Figure 3 exemplarily shows a cutting force F_c profile of a planing process in which a width of cut of a_e = 0.005 µm was selected.

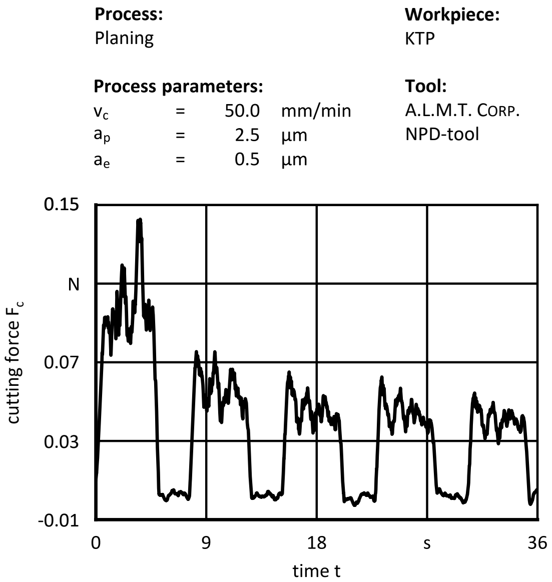

Figure 3. Measured cutting force F_c during full cut and partial cut conditions

In the first planing cycle, maximum cutting forces of $F_{c,max}$ = 0.122 N were identified. In the subsequent planing cycles, the cutting force decreases to an average value of F_c = 0.044 N. This behaviour is attributed to the larger chip cross-section A present during full-cut conditions compared to the subsequent partial-cut cycles. Finally, the comma-shaped chip formation region represents the area generated during the last planing cycle. It can be observed that fractures become more pronounced towards the groove edge in the direction of the width of cut a_e, which was consistently observed for all grooves. Therefore, this region can be considered the origin of fracture formation. This is consistent with the model proposed by BLAKE AND SCATTERGOOD [5], as the critical undeformed chip thickness h_{crit} is consistently exceeded in the upper region of the comma-shaped chip thickness distribution.

In general, ductile machining refers to a plastic material removal process with plastic chip formation, in which crack formation is prevented, thereby suppressing brittle fractures. Accordingly, the topographical analysis shown in Figure 4 reveals a significant decrease in the number of fractures n_f within the partial-cut region with decreasing width of cut a_e, indicating an increasing dominance of ductile-like machining mechanisms. However, it is noticeable that the fracture width w_f does not decrease linearly. Exemplarily, for a width of cut of a_e = 5 µm, fracture widths of w_f < 12 µm were identified, whereas for reduced widths of cut of a_e = 2 µm and a_e = 0.5 µm, fracture widths of $w_f \leq$ 8.5 µm and $w_f \leq$ 5.3 µm were observed within the partial-cut region, respectively. However, even at the smallest width of cut a_e = 0.5 µm within the selected process range, fractures could still be observed. Due to the statistical nature of brittle fractures, it cannot be excluded that neighbouring micro-cracks accumulate, causing the initial crack depth y_c to exceed the critical crack depth $y_{c,crit}$ and propagate to the surface. Consequently, individual fractures and micro-cracks remain in the following planing cycle with. This implies that the width of cut a_e influences the extent and probability of fractures, as evidenced by reductions in fracture width w_f and the number of fractures n_f. This indicates that more than a single planing pass is required to completely prevent fractures of this type.

Figure 5 shows the arithmetic mean height Sa and the arithmetic mean deviation Ra in relation to the width of cut a_e. A range of arithmetic mean heights of 0.89 nm ≤ Sa ≤ 11.97 nm and arithmetic mean deviations of 0.76 nm ≤ Ra ≤ 2.73 nm can be determined. It becomes evident that, initially starting from a width of cut of a_e = 0.5 µm, the arithmetic mean height decreases to Sa = 0.89 nm at a width of cut of a_e = 1.5 µm and subsequently increases to Sa = 11.97 nm up to a width of cut of a_e = 5 µm. A comparable trend is observed for the arithmetic mean deviation Ra.

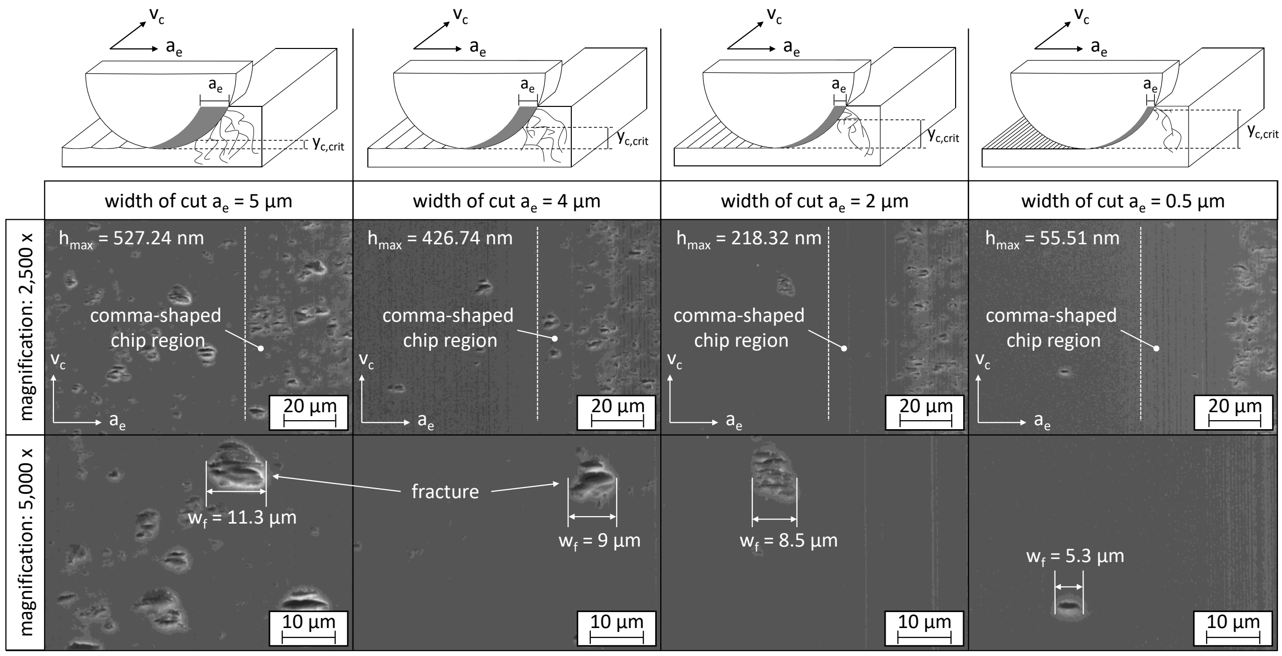

Figure 4. SEM images of crack formation at different widths of cut a_e and magnifications in the partial-cut region

The first reduction can be explained by the fact that, with a decreasing width of cut a_e, the maximum undeformed chip thickness h_{max} is reduced and the region of minimum chip thickness h_{min} shifts towards the main cutting edge S. This means that the achieved maximum chip thickness h_{max} approaches the value of the minimum chip thickness h_{min}, resulting in a higher theoretical roughness depth R_{th} and thus a higher arithmetic mean height Sa and arithmetic mean deviation Ra respectively [10]. This effect is further intensified by the higher cutting edge radius of a NPD-tool with $r_\beta < 1$ µm compared to a single-crystalline diamond tool with a cutting edge radius in the range of 20 nm ≤ r_β ≤ 50 nm [11]. The subsequent increase in the arithmetic mean height Sa and arithmetic mean deviation Ra is attributed to the more pronounced width-of-cut-related marks. Thus, the best surface quality in terms of arithmetic mean height within the selected process range can be identified at a width of cut of a_e = 1.5 µm with an arithmetic mean height of Sa = 0.89 nm and an arithmetic mean deviation of Ra = 0.76 nm.

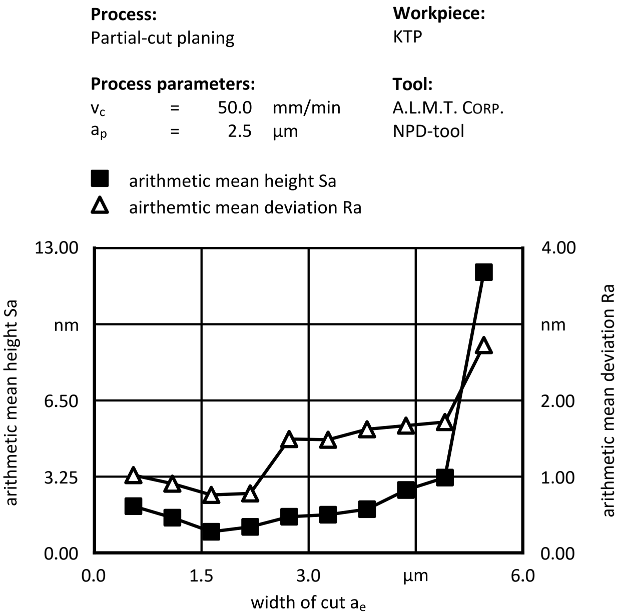

Figure 5. Influence of the width of cut a_e on the arithmetic mean height Sa

However, if fracture widths w_f are included in the surface evaluation, a reduction in fracture width with decreasing width of cut a_e can be observed. This trend is shown in Figure 6 by a linear regression of fracture width w_f versus width of cut a_e.

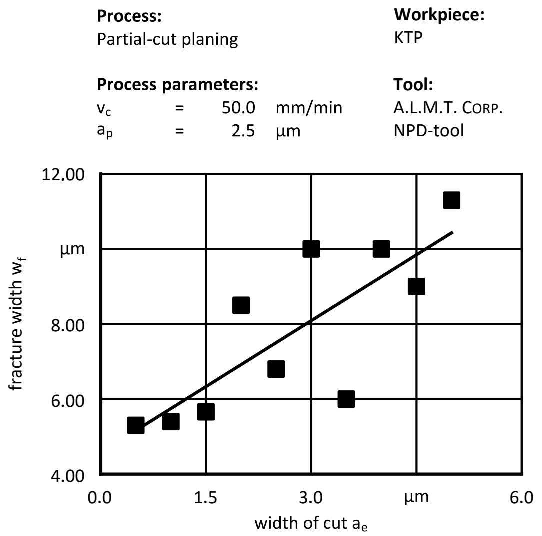

Figure 6. Influence of the width of cut a_e on the fracture width w_f

4. Conclusion

In this study, the influence of the width of cut a_e on surface generation during the machining of KTP was investigated. The results showed that the number of fractures n_b can be significantly reduced with a decreasing width of cut a_e. Within the width of cut range of 0.5 µm ≤ a_e ≤ 4.5 µm, arithmetic mean heights of Sa ≤ 3.21 nm and arithmetic mean deviations of Ra ≤ 1.72 nm could be achieved despite the presence of isolated fractures. However, the best surface qualities in terms of arithmetic mean height within the selected process range, characterized by 0.89 nm ≤ Sa ≤ 1.107 nm, were obtained within the width of cut range 1.5 µm ≤ a_e ≤ 2.0 µm. Consequently, for the planing process, the maximum undeformed chip thickness is within the range of 164.66 nm ≤ h_{max} ≤ 218.31 nm, in which ductile-like machining with an improved optical surface quality in terms of arithmetic mean height Sa can be achieved. If the undeformed chip thickness h is below the optimal range due to a reduced width of cut a_e, the surface quality deteriorates as a result of the increasing influence of the minimum chip thickness h_{min}. Conversely, if the maximum undeformed chip thickness h_{max} exceeds the optimal range due to a larger width of cut a_e, widths of cut marks are formed, which likewise impair the surface quality. Considering the fractures, it can be observed that decreasing the width of cut a_e leads to a consistent reduction in both the number of fractures n_f and the fracture width w_f.

Despite the reduced occurrence and extent of fractures, they were still present in every groove, indicating that fully ductile machining without fractures was not yet achieved.Therefore, these results provide the basis for further investigations into the influence of the rake angle γ_0 on ductile machining, as it represents an additional influencing parameter for the ductile machining of brittle materials.

References

[1] Lee S M, Kim H, Cha M and Moon H S: Polarization-entangled photon-pair source obtained via type-II non-collinear SPDC process with PPKTP crystal Optics Express 24, 2016, pp. 2,940 – 2,952.
[2] Guo J, Shi H and Pan B: Research on chemical mechanical polishing of KTiOPO4 crystal Proc. 8th Int. Conf. Nanomanufacturing and 4th AET Symp. ACSM and Digital Manufacturing 2022, (Nanoman-AETS), pp. 1 – 4.
[3] Rowe W B: Principles of Modern Grinding Technology Oxford. 2nd ed. Elsevier, 2014.
[4] Yan J, Yoshino M, Kuriagawa T, Shirakashi T, Syoji K and Komanduri R: On the ductile machining of silicon for micro electro-mechanical systems (MEMS), opto-electronic and optical applications Mater. Sci. Eng. A297, 2001, pp. 230 – 234.
[5] Blake P N, Scattergood R O: Ductile-Regime Machining of Germanium and Silicon J. Am. Ceram. Soc. 73, 1990, pp. 949 – 957.
[6] Uhlmann E, Polte M, Hocke T, Polte C, Polte J: Precise cutting of cemented carbide with nanopolycrystalline diamond in ductile regime euspen 23th Int. Con. and Exhib, 2023, pp. 1 – 2.
[7] Uhlmann E, Polte M, Hocke T, Wendt M, Polte C and Tschöpel J: Investigation of nanopolycrystalline diamond tools for ultra-precision machining of ppKTP-crystals for quantum communication applications euspen 25th Int. Con. and Exhib, 2025, pp. 1 – 2.
[8] Karlsson H and Laurell F: Electric field poling of flux grown KTiO4 Appl. Phys. Lett. 71, 1997, pp. 3,474 – 3,476.
[9] Bulla B: Ultrapräzisionszerspanung von Nanokorn-Hartmetall mit monokristallinen Diamantwerkzeugen Dissertation, RWTH Aachen, Aachen, 2013.
[11] Uhlmann E: Paris. 5th Meeting of the Collaborative Working Group on Micro Production Engineering CIRP Winter Meeting, 2014.
[10] Brammertz P H: Die Entstehung der Oberflächenrauheit beim Feindrehen Industrie-Anzeiger, 1961, pp. 25 – 32.